Chalcogenide Letters Vol. 6, No. 5, May 2009, p. 213 - 218

STRUCTURAL AND OPTICAL PROPERTIES OF NANOCRYSTALLINE $Se_{0.8}Te_{0.2}$

M. A. MAJEED KHAN*, M. WASI KHAN
King Abdullah Institute for Nanotechnology, P.O. Box 2454, King Saud University, Riyadh- 11451, Kingdom of Saudi Arabia

Nanocrystalline $Se_{0.8}Te_{0.2}$ films were grown on quartz substrates by using thermal evaporation technique. Structural and optical properties of as-grown and annealed samples were investigated with XRD, SEM and UV-visible spectroscopy. The x-ray diffraction pattern at room temperature shows that the sample are formed in single phase with monoclinic crystal symmetry having space group C*m*. Surface morphology of the glass as-grown film was investigated via scanning electron microscopy (SEM). The typical diameter of as-grown nanocrystalline sample is found to be 50 nm, which is consistent with crystallite size calculated by XRD data using Scherrer equation. The UV-visible absorption spectra of the nanocrystals show that the optical band gap of as-grown and annealed samples are situated systematically in the range of 2.10 - 1.95 eV, which is quite larger than the bulk phase of the materials. The results have been explained on the basis of the close interplay between the structural and optical properties.

(Received April 1, 2009; accepted May 3, 2009)

Keywords: Nanocrystalline, XRD, SEM, Optical band gap

1. Introduction

Nanoscience and nanotechnology includes the areas of synthesis, characterization, exploration, and application of nanostructured and nanosize materials. The great importance and interest for the nanostructured materials have driven pure science and applied research over the last few years [1–6]. Synthesis of nanomaterials [1–6] becomes more demanding day by day and the efforts to make these materials in large quantities and at low cost is moving at an even greater pace. It is now well established that the bulk properties of a material both electronic and physical largely depend on the size and it develops gradually with size [1]. Hence, a study of finite size effects on the material properties is of importance for scientific understanding as well as tailoring the particular application of those materials [2]. Nanoparticles and nanostructural materials represent an evolving technology that has an impact on an incredibly wide number of industry and markets. Recently, much interest has been focused on semiconductor nanocrystals because they exhibit strongly size-dependent optical and electrical properties. These characteristics open new applications including high performance optoelectronic devices [7]. The manufacture of nanoparticles can be achieved through a number of different techniques including colloidal methods, rf sputtering, molecular-beam epitaxy [7], pulsed laser deposition [8] and inert gas condensation (IGC) [9]. Selenium tellurium semiconductors have been a subject of interest in thin films form because of their properties that make them attractive for device application [10-11].

The aim of this work is to synthesize nanocrystalline materials of $Se_{0.8}Te_{0.2}$ sample using the thermal evaporation technique and characterize their structural, optical and electrical properties for functional nanodevice applications.

2. Experimental

The $Se_{0.8}Te_{0.2}$ nanostructured films were prepared by thermal evaporation technique. The films were grown on quartz substrates at room temperature (305K). In this method, 99.999% pure $Se_{0.8}Te_{0.2}$ powder was thoroughly mixed by grinding them with pestle and mortar. Direct evaporation of the mixture in powder form resulted in spattering of the powder when the boat is heated. Hence, the mixtures were made into pellets using hydraulic press with 3 MPa. Only in pellet form it was possible to evaporate the material completely. During the process, the substrate is cooled to a temperature of 77 K using liquid nitrogen. The source material is kept in a molybdenum boat placed at a suitable distance from the substrate. . The depositions were carried out in a high vacuum system having diffusion pump backed by rotary pump and with liquid nitrogen trap. Coatings were carried out in the pressure range of 2×10^{-6} mbar. A radiant heater was used to heat the substrate and the thickness of the films was monitored using a quartz crystal thickness monitor. A temperature controller was employed to control the substrate temperature with an accuracy of ±2° C. The as-grown films were annealed in vacuum (10^{-5} mbar) at two different temperatures, at 325 K and 375 K for 10 minutes. The optical transmission (%T) and reflectance (%R) of the films were measured using a double beam UV-VIS spectrophotometer (Camspec 550) in the wavelength range 350-900 nm at room temperature. The structural characterization was carried out by taking XRD pattern of the films at room temperature with the help of Philips x-ray diffractometer using CuK_{α} (λ=1.54056 Å) radiations as x-ray source.

3. Results and discussion

3.1 Structural characterization

The surface morphology of as-grown $Se_{0.8}Te_{0.2}$ thin film grown on quartz substrates has been examined by using scanning electron microscopy (SEM) and shown in Fig. 1. It is evident that the material exhibits spherical morphology and good monodispersity with diameter about 50 nm. Moreover, particles has well-defined spherical shaped with poor inter-grain connectivity over the scanned area of the film. The structure of $Se_{0.8}Te_{0.2}$ nanocrystalline is uniform and monodisperse. The shell of the single nanospheres is smooth and homogeneous, and only some little nanoparticles can be seen on the surface. The average particle sizes of the aggregated nanocrystalline samples were estimated by considering the minimum and maximum diameter of large number of particles and are given in Table 1 and the particle size are found to be in the range of 24–51 nm. Fig. 2 shows the experimental XRD pattern for $Se_{0.8}Te_{0.2}$ film before annealing. The analysis of XRD patterns at room temperature shows that the samples are formed in single phase. All of the peaks in this pattern can be indexed with monoclinic crystal symmetry having space group Cm, which is in agreement with the results reported earlier. There is no extra impurity peak was found. Table 1 indicates the (hkl) values, interplanar spacing, 2θ and intensity of corresponding peaks of the film by using PowderX software. It is clear from the table that calculated and experimental values are very well matched. The XRD patterns of other films show almost similar trends (not shown here). Based on the XRD pattern, the average particle size (t) of the as-grown nanospheres is estimated according to Scherrer's equation [12]:

$$t = \frac{k\lambda}{\beta \cos\theta} \tag{1}$$

where k (0.94) is a constant related to the indices of reflecting plane, λ is the wavelength of x-ray (1.5414Å), β is full width at half maximum (FWHM) of the diffraction peak (in radian) and 2θ is the angle of diffraction. The average grain size corresponding to the highest peak observed in XRD of as-grown and annealed films are found to be 51nm and 24 nm respectively. The presence of sharp structural peaks in XRD patterns and average grain size less 50 nm confirmed the nanocrystalline nature of the samples. However, no significant improvement in crystallinity and no

additional peak were observed after thermal annealing in vacuum at 325 K for 10 minutes and at 375 K for 15 minutes. The films exhibit reduction in the average grain size from ~51 to ~30 nm after first annealing and from ~30 to ~24 nm after the second annealing. These XRD results are in well agreement of SEM measurements at room temperature.

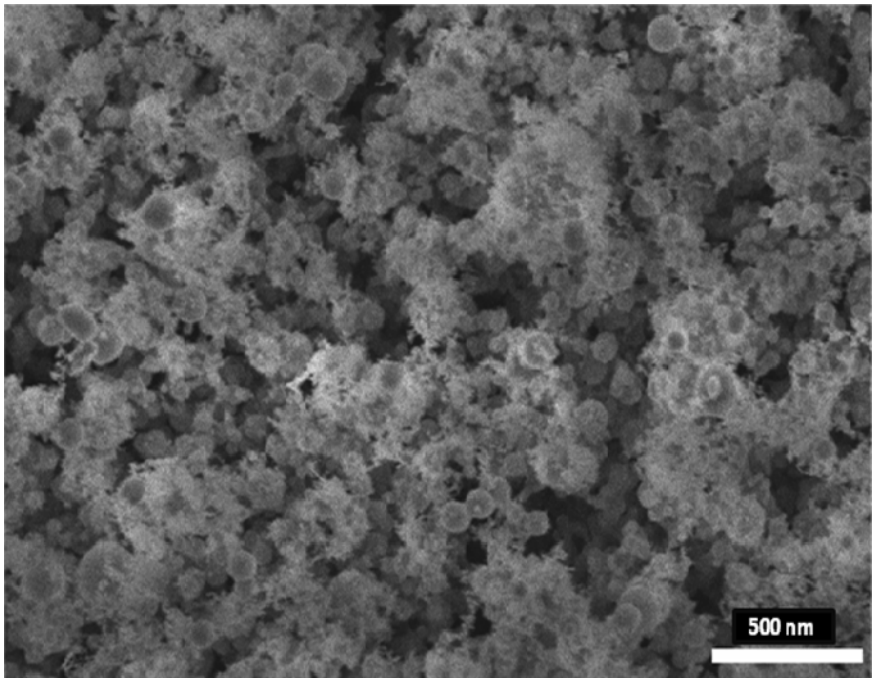

Fig. 1 Typical SEM micrograph of as-grown $Se_{0.8}Te_{0.2}$ nanosphere.

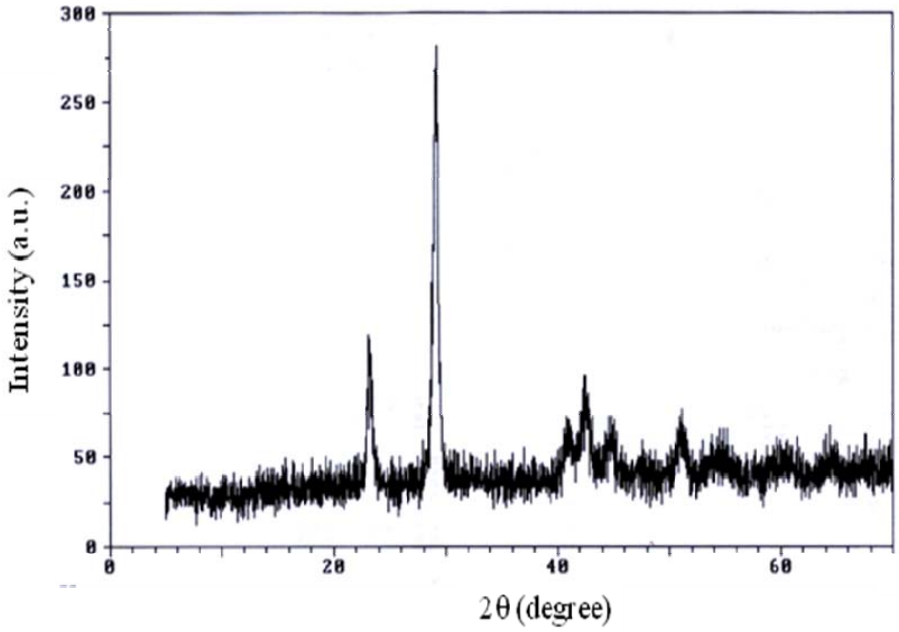

Fig. 2. X-ray diffraction pattern of as grown $Se_{0.8}Te_{0.2}$ thin film.

Table 1. Some important estimated parameters of $Se_{0.8}Te_{0.2}$ thin films from XRD data.

h	k	l	2θ (Obs.)	2θ (Cal.)	2θ (Diff.)	d (Obs.)	d (Cal.)	d (Diff.)	Intensity
0	1	2	23.222	23.249	-0.027	3.8272	3.82287	0.00433	118.72
1	3	0	29.254	29.258	-0.004	3.05035	3.04997	0.00038	268.25
-3	2	2	41.041	41.035	0.006	2.19745	2.19774	0.00029	65.64
2	0	3	42.758	42.765	0.007	2.02772	2.02517	0.00255	75.64
1	3	3	45.12	45.126	-0.006	2.0078	2.00754	0.00026	69.42
0	5	1	51.015	51.021	-0.012	2.47185	2.47103	0.00082	41.82
-4	8	0	54.82	54.81	0.01	1.67329	1.67357	0.00028	58.86
-1	6	4	59.703	59.699	0.004	1.54755	1.54765	0.0001	49.55
-5	1	2	60.497	68.491	0.006	1.36873	1.36883	0.0001	46.36
0	4	5	64.024	64.918	0.006	1.43515	1.43527	0.00012	49.3

3.2 Optical characterization

The optical studies of $Se_{0.8}Te_{0.2}$ films on the quartz substrates are carried out in the wavelength range of 350 to 900 nm at room temperature.

The transmission and reflection data were used to calculate absorption coefficient of the films at different wavelengths. The absorption coefficient, α, is given by the relation [13],

$$T = (1 - R)e^{-\alpha d} \tag{2}$$

where the thickness (d) of the $Se_{0.8}Te_{0.2}$ film is about 300 nm.

In order to determine the clear fundamental absorption edge, we have performed UV-visible absorption spectroscopy before and after annealing to study the variation of band gap E_g in the film. The energy gap E_g can be determined by [14]:

$$(\alpha h\nu)^n = A(h\nu - E_g) \tag{3}$$

where A is a constant and n characterizes the transition process. We can see n = 2 and 2/3 for direct allowed and forbidden transitions, respectively, and n = 1/2 and 1/3 for indirect allowed and forbidden transitions, respectively.

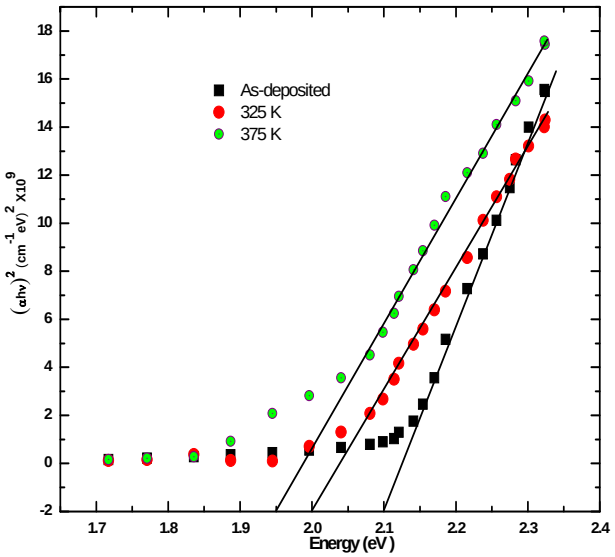

Fig. 3. UV-visible absorption spectra of as-grown and annealed films of $Se_{0.8}Te_{0.2}$ at room temperature.

Table-2. Values of band gap and particle size of as-grown and at annealed temperatures

Temperature (K)	E_g (eV) (± 0.01)	Particle size(nm)
As-grown	2.10	51-30
Annealed at 325 K	2.00	51-30
Annealed at 375 K	1.95	30-24

Fig. 3 shows curves of $(\alpha hv)^2$ versus hv (wavelength range 350-900 nm) obtained at room temperature of as-grown and annealed $Se_{0.8}Te_{0.2}$ thin films of thickness 3000Å. The curve has a good straight line fit over higher energy range above the absorption edge, indicative of a direct optical transition near the absorption edge. Based on Fig. 3, the direct energy gap E_g of the sample has been calculated and shown in Table 2. From figure it is observed that with increase in the annealing temperature, the slope is decreasing showing the corresponding decrease in the band gap of the film material. The blue shift in band gap is because of the reduction in grain size from ~51 to ~30 nm and then from ~30 to ~24nm. Clearly, the observed values of E_g are higher than the value of bulk optical gap of $Se_{0.8}Te_{0.2}$ due to quantum confinement in the $Se_{0.8}Te_{0.2}$ nanocrystallites. The change in optical band gap on increase in the annealing temperature may be due to a decrease of disorder in the materials and decrease in the density of defect states.

4. Conclusion

The present investigation demonstrates the variation in the structural and optical properties of as-grown and annealed $Se_{0.8}Te_{0.2}$ thin films. For this aim, $Se_{0.8}Te_{0.2}$ nanospheres of size 50 nm were grown on quartz substrates by thermal evaporation technique. The XRD pattern was indexed to the monoclinic structure and the average grain size estimated from the Scherrer's formula was around 51 nm. The optical band gap of films has been determined from the transmittance and reflectance spectra taken with the help of spectrophotometer in the wavelength range of 350-900 nm at room temperature. The results of UV-visible absorption spectroscopy also show the

systematic variation towards blue shift of band gap with increase in annealing temperature. This is due to the reduction in average particle size from ~51 to ~24 nm with increase in annealing temperature. The correlation between the structural and optical properties in the present system proves that the material is useful for nanotechnology applications.

References

[1] Alivisatos, A.P. Semiconductor clusters, nanocrystals, and quantum dots. Science **271**, 933(1996).

[2] Li, L.S.; Hu, J.T.; Yang, W.D.; Alivisatos, A.P. Band gap variation of size- and shape-controlled colloidal CdSe quantum rods, Nanoletters **1**(7), 349 (2001).

[3] Iijima, S. Helical microtubules of graphitic carbon. Nature **56**, 345 (1991).

[4] Duan, X.; Lieber, C.M. Laser-assisted catalytic growth of single crystal GaN nanowires. J. Am. Chem. Soc., **122**(1),188 (2000).

[5] Catherine, J.; Nikhil, R.J. Controlling the aspect ratio of inorganic nanorods and nanowires. Advanced Materials, **14**, 80 (2002).

[6] Su-Yuan, X.; Chun-Fang, W.; Xian-Hua, Z.; Zhi-Yuan, J.; Zhao-Xiong, X.; Zhong-Qun, T.; Rong-Bin, H.; Lan-Sun, Z. Spontaneous transformation of selenium from monoclinic microballs to trigonal nano-rods in ethanol solution. J. Mater. Chem., **13**, 1447 (2003).

[7] L. E. Brus, A. Efros and T. Itoh, J. Lumin., **76**, 1 (1996).

[8] Xu NingBoo and Bong Hyun, Semi. Sci. and Tech., **18**, 300 (2003).

[9] R. Birringer, H. Gleiter, H. P. Klein and P. Marquardt, Phys. Lett., **102A**, 365 (1984).

[10] K. Yilmaz M. Parlak and C. Ercelebi J. Mater. Sci. Mater. Electronics **10,** 225 (2004).

[11] C. Amory, J. C. Bernede, E. Halgand and S. Marsillac **431-432**, 22 (2003).

[12] B. D. Cullity, Elements of x-ray diffraction, Addison-wesley, 1978.

[13] H. Kim, C. M. Gilmore, A. Pique, J. S. Horwitz, H. Mattoussi, H. Murata, Z. H. Kafafi, D. B. Chrisey,J. Appl. Phys. **86**(11), 6451 (1999).

[14] J. Tauc, Amorphous and Liquid Semiconductors, Plenum, New-York 159, 1974.